Thermodynamics of Binding Between Proteins and Carbon Nanoparticles: The Case of C60@Lysozyme

Thermodynamics of Binding Between Proteins and Carbon Nanoparticles: The Case of C60@Lysozyme

Matteo Calvaresi[*†], Andrea Bottoni[†], and Francesco Zerbetto[†]

[†] Dipartimento di Chimica "G. Ciamician", Alma Mater Studiorum, Università di Bologna, via F. Selmi 2, 40126 Bologna, Italy

J. Phys. Chem. C, 2015, 119 (50), pp 28077–28082
DOI: 10.1021/acs.jpcc.5b09985
Publication Date (Web): November 18, 2015
Available at: https://pubs.acs.org/doi/full/10.1021/acs.jpcc.5b09985

Thermodynamics of Binding Between Proteins and Carbon Nanoparticles: The Case of C_{60}@Lysozyme

Matteo Calvaresi,[†,*] *Andrea Bottoni,*[†] *Francesco Zerbetto*[†]

[†] Dipartimento di Chimica "G. Ciamician", Alma Mater Studiorum – Università di Bologna, via F. Selmi 2, 40126 Bologna, Italy

ABSTRACT. The analysis of the interaction between C_{60} and lysozyme provides general rules to identify the forces that govern the thermodynamics of binding between proteins and carbon nanoparticles. The main driving force of the binding are van der Waals interactions. Polar solvation and entropy, contributions that are often neglected, are strongly detrimental to the binding. These energetically relevant terms must be taken into account when protein/CNPs hybrids are designed.

INTRODUCTION

The integration of carbon nanoparticle (CNPs) with proteins to form hybrid functional assemblies is an innovative research area with promise for medical, nanotechnological, and materials science applications.[1-7] The specifics of molecular recognition and catalytic activity of proteins combined with the peculiar chemical-physics properties of CNPs provides opportunities to develop new nanomachines, sensors and theranostic platforms.[1-7] The ability of CNPs to interact with proteins was demonstrated for the first time by pioneering work that reported the C_{60} inhibiting activity on HIV-proteases.[8] Protein interactions with fullerene-based compounds were later identified in many other systems both experimentally[9-27] and computationally.[3,28-40]. It is generally hard to ascertain if the protein-CNP interactions result in (i) formation of a well-defined stoichiometric adduct, (ii) binding of the protein with CNPs aggregates, or (iii) average effects due to binding of CNPs to multiple protein binding sites. Recently, NMR chemical shift perturbation analysis identified unambiguously a CNP-protein binding pocket in solution.[41] The NMR and spectroscopic data showed unequivocally that lysozyme forms a stoichiometric 1:1 adduct with C_{60} where lysozyme maintains its tridimensional structure with only a few well-identified residues that are structurally perturbed.[41] The C_{60} binding pocket is highly specific and localized in the catalytic site of the protein.[41] In spite of these very important structural data little is known about the thermodynamics of binding between proteins and carbon nanoparticles. Molecular dynamics (MD) simulations have already provided precious information regarding interactions of CNPs with proteins showing the dynamics at the molecular level and addressing the effects of surface chemistry on the adsorption of proteins.[28-48] The intent of this work is to lay the ground for a computational approach able to identify the thermodynamics contributions responsible for the interaction between proteins and CNPs. The analysis of the energy

contributions to the binding between lysozyme, usually considered the ideal workhorse to study protein-CNP hybrid systems,[21,41,46-53] and C_{60} can supply guidelines for the general applicability and understanding of protein–CNP interactions.

COMPUTATIONAL DETAILS

Setting the simulation.

Experimental restraints data from NMR and a docking protocol[3,28,36,41,46,54] recently validated for the study of interaction between proteins and nanoobjects were used to generate the initial coordinates of the adduct between protein and C_{60}. Using ^{1}H,^{15}N HSQC NMR spectra the most perturbed amide NH groups of the protein backbone were identified. The residues that undergo the largest changes cluster in a specific region of the three-dimensional structure of the protein that we identified as the fullerene binding pocket. We cannot exclude that other residues participate to the binding, because in the NMR study we investigated only the perturbation of NH amidic bonds. Other residues can interact with their side chains. For this reason we carried out MD simulations to study the interaction of the amino acid side chains of lysozyme with the C_{60} cage. Chloride counterions were included to exactly neutralize the positively charged lysozyme. All simulations were performed with explicit solvent by using the TIP3P water model (7605 water molecules).[57] The ff10 force field was used to model lysozyme.[56] The C_{60} atoms were modeled as uncharged Lennard–Jones particles by using sp2 carbon parameters from the ff10 force field.[56]

Minimization and equilibration.

About 1000 steps of steepest descent minimization were performed with SANDER.[56] The minimized structure (only cleared from severe sterical clashes) was considered for a 3 step

equilibration protocol. Particle Mesh Ewald summation[56] was used throughout (cut off radius of 10 Å for the direct space sum). H-atoms were considered by the SHAKE algorithm[56] and a time step of 2 fs was applied in all MD runs. Individual equilibration steps included (i) 50 ps of heating to 298 K within an NVT ensemble and temperature coupling according to Berendsen.s1 (ii) 50 ps of equilibration MD at 298 K to switch from NVT to NPT and adjust the simulation box. Isotropic position scaling was used at default conditions. (iii) 400 ps of continued equilibration MD at 298 K for an NPT ensemble switching to temperature coupling according to Andersen.

Production MD.

MD simulation was carried out for the equilibrated system using SANDER.[56] Simulation conditions were identical to the final equilibration step (iii). Overall sampling time was 100 ns. Snapshot structures were saved into individual trajectory files every 1000 time steps, i.e. every 2 ps of molecular dynamics.

Post processing of trajectories, MM-PBSA Molecular Mechanics/ Poisson Boltzmann (or Generalized Born) Surface Area.

MM/PB(GB)SA calculations is a post-processing method in which representative snapshots from an ensemble of conformations are used to calculate the free energy change between two states (typically a bound and free state of a receptor and a ligand).[56,57] Free energy differences are calculated by combining the gas phase energy contributions that are independent of the solvent model as well as solvation free energy components (both polar and non-polar) calculated from an implicit solvent model for each species.[58] The molecular mechanics energies are determined with the SANDER[57] program from Amber and represent the internal energy (bond, angle and dihedral), and van der Waals and electrostatic interactions. An infinite cutoff for all interactions

is used. The electrostatic contribution to the solvation free energy is calculated with a numerical solver for the Poisson-Boltzmann (PB) method, as implemented in the PBSA programs[56,57] or by generalized Born (GB) methods implemented in SANDER.

The nonpolar contribution to the solvation free energy has been determined with solvent-accessible surface-area dependent terms. Individual snapshot structures of all trajectories were analyzed with program PTRAJ.[56] MMPBSA[56,57] analysis was carried out to estimate the binding free energy of the C_{60} when complexed to Lysozyme. Continuum solvation contributions were estimated by either using the PB or the GB module.[56,57] To obtain an estimate of the binding entropy, the normal modes for the complex, receptor and ligand are calculated and the results are averaged, using the PTRAJ program[56] (Normal Mode Analysis) via MMPBSA.py.[58]

RESULTS AND DISCUSSIONS

Starting from the NMR data,[41] the geometry of C_{60}-lysozyme complex was built. Subsequently, 100 ns of molecular dynamics simulations were carried out (see Computational Details). To estimate the binding energy between lysozyme and C_{60}, a molecular mechanics/Poisson–Boltzmann Surface Area (MM-PBSA) analysis of the trajectories was finally performed.[57] The interaction energy ($\Delta G_{binding}$) between C_{60} and lysozyme is -18.5 kcal mol^{-1}.

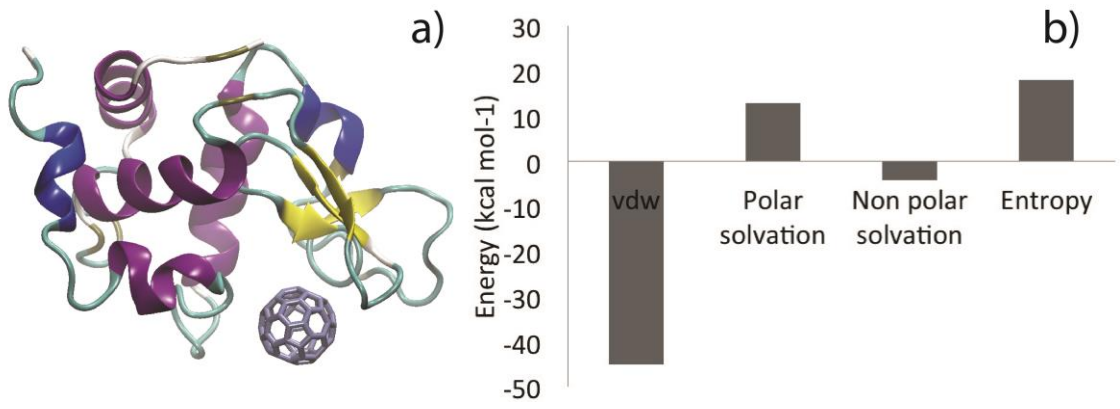

Figure 1. a) Binding pocket of C_{60} in lysozyme. b) Energy components of $\Delta G_{binding}$

Analysis of the binding components of the energy (Figure 1) shows that van der Waals interactions are the driving force to the binding (-45.1 kcal mol^{-1}). Hydrophobic interactions, i.e. non-polar solvation, assist the binding, even if the corresponding value (-4.3 kcal mol^{-1}) is far smaller than that of the vdW interactions. Interestingly, polar solvation and entropy are detrimental to the binding and their contribution is positive. The entropic term is often neglected when protein-CNPs interactions are analyzed because of the rigidity of the CNPs. However, this term, which is here estimated at 18.1 kcal mol^{-1}, is energetically relevant and should be taken into account when protein-CNPs hybrids are designed. This large value arises from the fact that binding of C_{60} to the protein cavity causes a marked decrease in amino acid mobility:[28] as C_{60} approaches its binding site, protein residues stick to its surface to maximize vdW interactions and become glued to the fullerene cage.[28] The polar solvation term (12.8 kcal mol^{-1}) is also rather important and deserves an accurate analysis. We carried out a decomposition analysis of the trajectory according to the MM-PBSA scheme[57,58] and obtained the contribution to the binding of each amino acid.

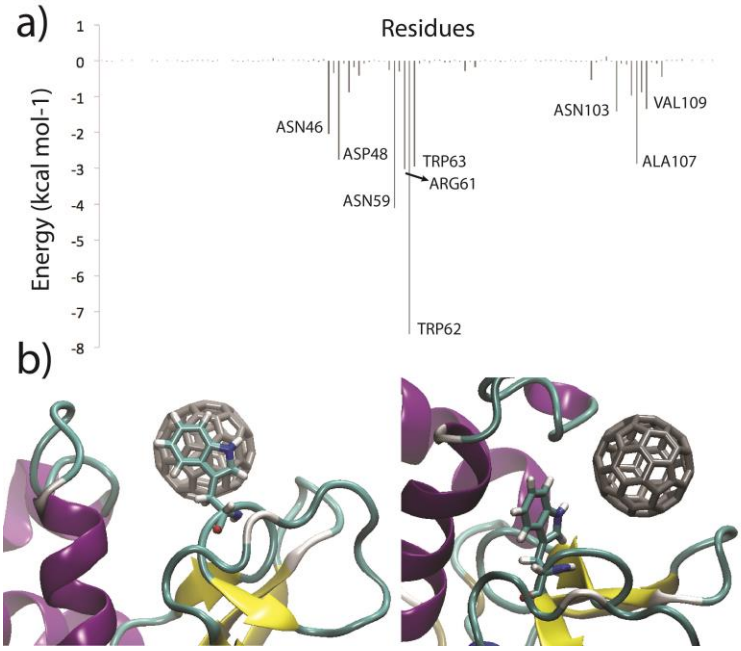

Figure 2. a) Lysozyme/C_{60} interactions. $\Delta G_{binding}$ decomposed per residue. b) Interaction between Trp62, Trp 63 and C_{60}.

Figure 2 emphasizes the role of Trp residues in the binding process (Trp62 and Trp63). Experimentally, Trp fluorescence is almost completely quenched upon C_{60} binding, confirming the important role of Trp residues.[41] Protein adsorption onto CNPs improves with the increase of the content of aromatic residues in the protein sequence.[60-63] Among the aromatic amino acids, tryptophan possesses the highest affinity for CNPs, followed by tyrosine, phenylalanine, and histidine.[60-63] π-stacking contacts between the indolic group of Trp residues and the cage of the CNPs, which is sandwich-like for Trp62 and T-shaped-like for Trp63, govern the interactions, as shown in Figure 2. A crucial role in the binding of lysozyme to C_{60}, and in general of proteins to CNPs, is played by amphiphilic residues such as glutamine, asparagine, aspartic acid, glutamic acid, arginine and lysine that quantitatively provide significant contributions (Figure 2).

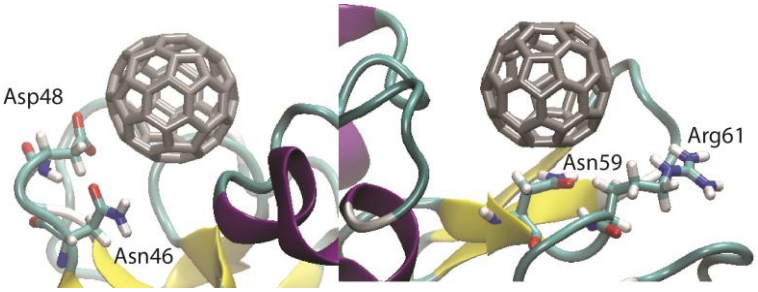

Figure 3. Interaction between Asn59, Arg61, Asn46 and Asp48 with C_{60}.

Inspection of the binding mode of Asn46, Asp48, Asn59, and Arg61 (Figure 3) shows that the hydrophobic methylenic groups of these residues interact with C_{60}, whereas the hydrophilic groups point toward the water environment. This behavior is similar to that of the hydrophilic head of a surfactant, generating surfactant-like interactions,[4,46] whose importance was also independently confirmed by other groups studying protein-CNP interactions.[1-7,64-67] Purely hydrophobic residues, such as Ala107 and Val109, play an important role *via* vdW interactions and hydrophobic effects (Figure S1). The per-residue decomposition of $\Delta G_{binding}$ helps understanding the chemical origin of the various contributions. The vdW components, which follow the global $\Delta G_{binding}$ decomposition (see Figure S2 and Figure S3), play the most important role in the binding between lysozyme and C_{60} and govern, in general, the recognition and binding processes between proteins and CNPs. We recently demonstrated that the interaction between C_{60} and K^+ channels is exclusively controlled by shape complementarity and, as a consequence, by vdW interactions.[28] This phenomenon resembles the well-known encapsulation of pristine C_{60} molecules by macrocyclic receptors,[68,69] where concave–convex complementarity is the driving force to the binding.[70]

We also analyzed the effect of CNP binding in terms of solvation contributions. Perhaps naively, it is reasonable to expect that moving a CNP from aqueous solution toward a protein

binding pocket should be a favored process. Actually, polar (12.8 kcal mol^{-1}) and non-polar (-4.3 kcal mol^{-1}) solvation energies have opposite trends (Figure 1). As hydrophobic C_{60} occupies the protein binding site, it sheds water molecules (hydrophobic effect), as underlined by the analysis of the Solvent Accessible Surface Area (SASA in Figure S4), with an energy gain of -2.4 kcal mol^{-1}(see Figure S5). This term, i.e., non polar solvation, takes into account, even if not entirely accurate, the entropy increase due to the water molecules in the first hydration shell that are tightly bound to the protein and are set free upon non-covalent interaction with the fullerene. The small variation of SASA during the MD suggests that C_{60} binds with a pre-formed pocket able to recognize the fullerene shape (Figure 4).

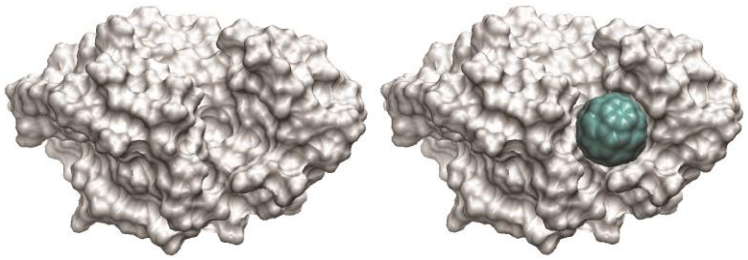

Figure 4. Surface complementarity between the protein and the C_{60} cage.

Smaller contributions for the non-polar solvation also originate from the hydrophobic parts (aliphatic chains) of some amino acids, that, upon C_{60} binding, come to be in contact with the hydrophobic surface of the C_{60} cage instead of water that interacts unfavorably with these regions (0.32 kcal mol^{-1} for Trp62, 0.24 kcal mol^{-1} for Ala107, 0.23 kcal mol^{-1} for Asp48 and 0.20 kcal mol^{-1} for Asn46). On the other hand the binding of CNPs usually occurs in substrate binding pockets (or channels), that are regions exposed to water and where amino acids with polar side groups are commonly located.

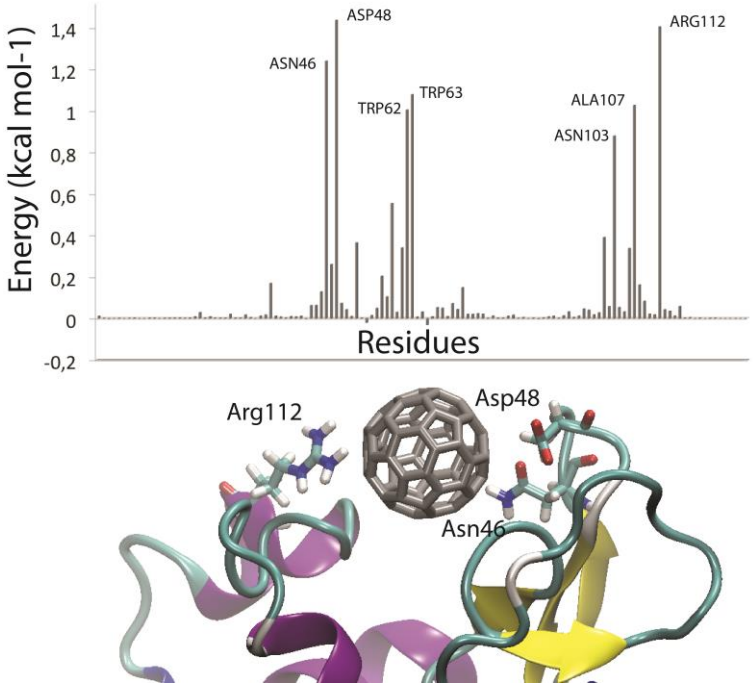

Figure 5. Contributions to polar solvation per residue.

The hydrophilic parts of these residues, upon formation of the complex with C_{60}, are forcedly desolvated, causing a destabilization of the system (Figure 5a). This is the case of the charged residues Asp48 or Arg112 (Figure 5b): these are less favored residues after interaction with C_{60}, because they are screened with respect to water molecules, thus reducing the corresponding solvation energy. These residues, in the presence of the hydrophobic C_{60} molecule, are no longer able to interact with water molecules usually present in the binding pocket. The various specific contributions are energetically relevant and the solvation energy of several residues decreases by more than 1 kcal mol^{-1} (Figure 5). The overall effect to solvation after C_{60} binding is that polar solvation effects overcome the non-polar ones and on the whole the binding is less favored. A crucial role of the solvation free energy was previously described also for thermodynamic stability of C_{60} and γ- cyclodextrin complex in aqueous solution.[71]

CONCLUSION

In conclusion, we described a computational procedure that provides a detailed analysis of the various components of the binding energy and quantify the protein-CNP interaction at the level of single residues. This approach allows to determine “hot” and “cold” spots for the protein-CNP interaction and to design new functionalization patterns of the CNPs or, alternatively, design protein mutants able to modulate their interactions with the CNP.

ASSOCIATED CONTENT

Supporting Information. Binding of C_{60} with Ala107 and Val109 (Figure S1); per residue decomposition total binding energy (Figure S2); per residue decomposition vdw binding energy (Figure S3); variation of SASA as a function of time (Figure S4); per residue decomposition non polar solvation energy (Figure S5).

AUTHOR INFORMATION

Corresponding Author

* MC: matteo.calvaresi3@unibo.it

ACKNOWLEDGMENTS

This study was supported by the Italian Ministry of Education, University and Research MIUR - SIR Programme no. RBSI149ZN9 – BIOTAXI funded to MC.

REFERENCES

(1) De Leo, F.; Magistrato, A.; Bonifazi, D. Interfacing Proteins with Graphitic Nanomaterials: From Spontaneous Attraction to Tailored Assemblies. *Chem. Soc. Rev.* **2015**, *44*, 6916-6953.

(2) Da Ros, T.; Prato, M. Medicinal Chemistry with Fullerenes and Fullerene Derivatives. *Chem. Commun.* **1999**, 663-669.

(3) Calvaresi, M.; Zerbetto, F. Baiting Proteins with C_{60}. *ACS Nano* **2010**, *4*, 2283-2299.

(4) Calvaresi, M.; Zerbetto, F. The Devil and Holy Water: Protein and Carbon Nanotube Hybrids. *Acc. Chem. Res.* **2013**, *46*, 2454-2463.

(5) Marchesan, S.; Prato, M. Under the Lens: Carbon Nanotube and Protein Interaction at the Nanoscale. *Chem. Commun.* **2015**, *51*, 4347-4359.

(6) Heister, E.; Brunner, E. W.; Dieckmann, G. R.; Jurewicz, I.; Dalton, A. B. Are Carbon Nanotubes a Natural Solution? Applications in Biology and Medicine. *ACS Appl. Mater. Interfaces* **2013**, *5*, 1870-1891.

(7) Nepal, D.; Geckeler, K. E. Proteins and Carbon Nanotubes: Close Encounter in Water. *Small* **2007**, *3*, 1259-1265.

(8) Friedman, S. H.; DeCamp, D. L.; Sijbesma, R. P.; Srdanov, G.; Wudl, F.; Kenyon, G. L. Inhibition of the HIV-1 Protease by Fullerene Derivatives. Model-Building Studies and Experimental Verification. *J. Am. Chem. Soc.* **1993**, *115*, 6506-6509.

(9) Pan, Y.; Wang, L.; Kang, S.; Lu, Y.; Yang, Z.; Huynh, T.; Chen, C.; Zhou, R.; Guo, M.; Zhao, Y. Gd-Metallofullerenol Nanomaterial Suppresses Pancreatic Cancer Metastasis by Inhibiting the Interaction of Histone Deacetylase 1 and Metastasis-Associated Protein 1. *ACS Nano* **2015**, *9*, 6826-6836.

(10) Zanzoni, S.; Ceccon, A.; Assfalg, M.; Singh, R. K.; Fushman, D.; D'Onofrio, M. Polyhydroxylated [60]Fullerene Binds Specifically to Functional Recognition Sites on a Monomeric and a Dimeric Ubiquitin. *Nanoscale* **2015**, *7*, 7197-7205.

(11) Miao, Y.; Xu, J.; Shen, Y.; Chen, L.; Bian, Y.; Hu, Y.; Zhou, W.; Zheng, F.; Man, N.; Shen, Y. et al. Nanoparticle as Signaling Protein Mimic: Robust Structural and Functional Modulation of CaMKII upon Specific Binding to Fullerene C60 Nanocrystals. *ACS Nano* **2014**, *8*, 6131-6144.

(12) Chen, P.; Seabrook, S. A.; Epa, V. C.; Kurabayashi, K.; Barnard, A. S.; Winkler, D. A.; Kirby, J. K.; Ke, P. C. Contrasting Effects of Nanoparticle Binding on Protein Denaturation. *J. Phys. Chem. C* **2014**, *118*, 22069;

(13) Mentovich, E.; Belgorodsky, B.; Gozin, M.; Richter, S.; Cohen, H. Doped Biomolecules in Miniaturized Electric Junctions. *J. Am. Chem. Soc.* **2012**, *134*, 8468-8473.

(14) Kang, S. G.; Zhou, G.; Yang, P.; Liu, Y.; Sun, B.; Huynh, T.; Meng, H.; Zhao, L.; Xing, G.; Chen, C. et al. Molecular Mechanism of Pancreatic Tumor Metastasis Inhibition by $Gd@C_{82}(OH)_{22}$ and its Implication for de novo Design of Nanomedicine. *Proc. Natl. Acad. Sci. U.S.A.* **2012**, *109*, 15431-15436.

(15) Zhen, M.; Zheng, J.; Ye, L.; Li, S.; Jin, C.; Li, K.; Qiu, D.; Han, H.; Shu, C.; Yang, Y. et al. Maximizing the Relaxivity of Gd-Complex by Synergistic Effect of HSA and Carboxylfullerene. *ACS Appl. Mater. Interfaces* **2012**, *4*, 3724-3729.

(16) Wu, H.; Lin, L.; Wang, P.; Jiang, S.; Dai, Z.; Zou, X. Solubilization of Pristine Fullerene by the Unfolding Mechanism of Bovine Serum Albumin for Cytotoxic Application. *Chem. Commun.* **2011**, *47*, 10659-10661.

(17) Ratnikova, T. A.; Govindan, P. N.; Salonen, E.; Ke, P. C. In Vitro Polymerization of Microtubules with a Fullerene Derivative. *ACS Nano* **2011**, *5*, 6306-6314.

(18) Maoyong, S.; Guibin, J.; Junfa, Y.; Hailin, W. Inhibition of Polymerase Activity by Pristine Fullerene Nanoparticles Can Be Mitigated by Abundant Proteins. *Chem. Commun.* **2010**, *46*, 1404-1406.

(19) Innocenti, A.; Durdagi, S.; Doostdar, N.; Strom, T. A.; Barron, A. R.; Supuran, C. T. Nanoscale Enzyme Inhibitors: Fullerenes Inhibit Carbonic Anhydrase by Occluding the Active Site Entrance. *Biorg. Med. Chem.* **2010**, *18*, 2822-2828.

(20) S. Durdagi, C. T. Supuran, T. A. Strom, N. Doostdar, M. K. Kumar, A. R. Barron, T. Mavromoustakos, M. G. Papadopoulos, In Silico Drug Screening Approach for the Design of Magic Bullets: a Successful Example with Anti-HIV Fullerene Derivatized Amino Acids. *J. Chem. Inf. Model.* **2009**, *49*, 1139-1143.

(21) Yang, S.-T.; Wang, H.; Guo, L.; Gao, Y.; Liu, Y.; Cao, A. Interaction of Fullerenol with Lysozyme Investigated by Experimental and Computational Approaches. *Nanotechnology* **2008**, *19*, 395101.

(22) Zhang, X.; Shu, C.; Xie, L.; Wang, C.; Zhang, Y.; Xiang, J.; Li, L.; Tang, Y. Protein Conformation Changes Induced by a Novel Organophosphate-Containing Water-Soluble Derivative of a C60 Fullerene Nanoparticle. *J. Phys. Chem. C* **2007**, *111*, 14327-14333.

(23) Pastorin, G.; Marchesan, S.; Hoebeke, J.; Da Ros, T.; Ehret-Sabatier, L.; Briand, J.-P.; Prato, M.; Bianco, A. Design and Activity of Cationic Fullerene Derivatives as Inhibitors of Acetylcholinesterase. *Org. Biomol. Chem.* **2006**, *4*, 2556-2562.

(24) Belgorodsky, B.; Fadeev, L.; Kolsenik, J.; Gozin, M. Formation of a Soluble Stable Complex between Pristine C_{60}-Fullerene and a Native Blood Protein. *ChemBioChem*, **2006**, *7*, 1783-1789.

(25) Belgorodsky, B.; Fadeev, L.; Ittah, V.; Benyamini, H.; Zelner, S.; Huppert, D.; Kotlyar, A. B.; Gozin, M. Formation and Characterization of Stable Human Serum Albumin−Tris-malonic Acid [C_{60}]Fullerene Complex. *Bioconjugate Chem.* **2005**, *16*, 1058-1062.

(26) Mashino, T.; Shimotohno, K.; Ikegami, N.; Nishikawa, D.; Okuda, K.; Takahashi, K.; Nakamura, S.; Mochizuki, M. Human Immunodeficiency Virus-Reverse Transcriptase Inhibition and Hepatitis C Virus RNA-Dependent RNA Polymerase Inhibition Activities of Fullerene Derivatives. *Bioorg. Med. Chem.* Lett. **2005**, *15*, 1107-1109.

(27) Park, K. H.; Chhowalla, M.; Iqbal, Z.; Sesti, F. Single-Walled Carbon Nanotubes are a New Class of Ion Channel Blockers. *J. Biol. Chem.* **2003**, *278*, 50212-50216.

(28) Calvaresi, M.; Furini, S.; Domene, C.; Bottoni, A.; Zerbetto, F. Blocking the Passage: C_{60} Geometrically Clogs K^+ Channels. *ACS Nano* **2015**, *9*, 4827-4834.

(29) Turabekova, M.; Rasulev, B.; Theodore, M.; Jackman, J.; Leszczynsk, D.; Leszczynski, J. Immunotoxicity of Nanoparticles: A Computational Study Suggests that CNTs and C_{60} Fullerenes Might Be Recognized as Pathogens by Toll-like Receptors. *Nanoscale* **2014**, *6*, 3488-3495.

(30) Radic, S.; Nedumpully-Govindan, P.; Chen, R.; Salonen, E.; Brown, J. M.; Ke, P. C.; Ding, F. Effect of Fullerenol Surface Chemistry on Nanoparticle Binding-Induced Protein Misfolding. *Nanoscale* **2014**, *6*, 8340-8349.

(31) Zuo, G.; Kang, S.-G.; Xiu, P.; Zhao, Y.; Zhou, R. Interactions Between Proteins and Carbon-Based Nanoparticles: Exploring the Origin of Nanotoxicity at the Molecular Level. *Small* **2013**, *9*, 1546-1556.

(32) Yang, S.-T.; Liu, Y.; Wang, Y.-W.; Cao, A. Biosafety and Bioapplication of Nanomaterials by Designing Protein-Nanoparticle Interactions. *Small* **2013**, *9*, 1635-1653.

(33) Govindan, P. N.; Monticelli, L.; Salonen, E. Mechanism of *Taq* DNA Polymerase Inhibition by Fullerene Derivatives: Insight from Computer Simulations. *J. Phys. Chem. B* **2012**, *116*, 10676-10683.

(34) Monticelli, L.; Barnoud, J.; Orlowskid, A.; Vattulainen, I. Interaction of C70 Fullerene with the Kv1.2 Potassium Channel. *Phys. Chem. Chem. Phys*. **2012**, *14*, 12526-12533.

(35) Kang, S. G.; Huynh, T.; Zhou, R. H. Non-Destructive Inhibition of Metallofullerenol $Gd@C_{82}(OH)_{22}$ on WW Domain: Implication on Signal Transduction Pathway. *Sci. Rep.* **2012**, *2*, 957.

(36) Calvaresi, M.; Zerbetto, F. Fullerene Sorting Proteins. *Nanoscale*, **2011**, *3*, 2873-2881.

(37) Zuo, G.; Zhou, X.; Huang, Q.; Fang, H.; Zhou, R. Adsorption of Villin Headpiece onto Graphene, Carbon Nanotube, and C60: Effect of Contacting Surface Curvatures on Binding Affinity. *J. Phys. Chem. C* **2011**, *115*, 23323-23328.

(38) Kraszewski, S.; Tarek, M.; Treptow, W.; Ramseyer, C. Affinity of C_{60} Neat Fullerenes with Membrane Proteins: A Computational Study on Potassium Channels. *ACS Nano* **2010**, *4*, 4158-4164.

(39) Wu, X.; Yang, S.-T.; Wang, H.; Wang, L.; Wang, L.; Hu, W.; Cao, A.; Liu, Y. Influences of the Size and Hydroxyl Number of Fullerenes/Fullerenols on their Interactions with Proteins. *J. Nanosci. Nanotechnol.* **2010**, *10*, 6298-6304.

(40) Benyamini, H.; Shulman-Peleg, A.; Wolfson, H. J.; Belgorodsky, B.; Fadeev, L.; Gozin, M. Interaction of C_{60}-Fullerene and Carboxyfullerene with Proteins: Docking and Binding Site Alignment. *Bioconjugate Chem.* **2006**, *17*, 378-386.

(41) Calvaresi, M.; Arnesano, F.; Bonacchi, S.; Bottoni, A.; Calo`, V.; Conte, S.; Falini, G.; Fermani, S.; Losacco, M.; Montalti, M. et al. C_{60}@Lysozyme: Direct Observation by Nuclear Magnetic Resonance of a 1:1 Fullerene Protein Adduct. *ACS Nano* **2014**, *8*, 1871-1877.

(42) Yao, K.; Tan, P.; Luo, Y.; Feng, L.; Xu, L.; Liu, Z.; Li, Y.; Peng, R. Graphene Oxide Selectively Enhances Thermostability of Trypsin. *ACS Appl. Mater. Interfaces* **2015**, *7*, 12270-12277.

(43) Calvaresi, M.; Zerbetto, F. Atomistic Molecular Dynamics Simulations Reveal Insights into Adsorption, Packing, and Fluxes of Molecules with Carbon Nanotubes *J. Mater. Chem. A* **2014**, *2*, 12123-21135.

(44) Sun, X.; Feng, Z.; Hou, T.; Li, Y. Mechanism of Graphene Oxide as an Enzyme Inhibitor from Molecular Dynamics Simulations. *ACS Appl. Mater. Interfaces* **2014**, *6*, 7153-7163.

(45) Akdim, B.; Pachter, R.; Kim, S. S.; Naik, R. R.; Walsh, T. R.; Trohalaki, S.; Hong, G.; Kuang, Z.; Farmer, B. L. Electronic Properties of a Graphene Device with Peptide Adsorption: Insight from Simulation. *ACS Appl. Mater. Interfaces* **2013**, *5*, 7470-7477.

(46) Calvaresi, M.; Hoefinger, S.; Zerbetto, F. Probing the Structure of Lysozyme–Carbon-Nanotube Hybrids with Molecular Dynamics. *Chem. Eur. J.* **2012**, *18*, 4308-4313.

(47) Balamurugan, K.; Singam, E. R. A.; Subramanian, V. Effect of Curvature on the α-Helix Breaking Tendency of Carbon Based Nanomaterials. *J. Phys. Chem. C* **2011**, *115*, 8886-8892.

(48) Zuo, G.; Gu, W.; Fang, H.; Zhou, R. Carbon Nanotube Wins the Competitive Binding over Proline-Rich Motif Ligand on SH3 Domain. *J. Phys. Chem. C* **2011**, *115*, 12322-12328.

(49) Du, P.; Zhao, J.; Mashayekhi, H.; Xing, B. Adsorption of Bovine Serum Albumin and Lysozyme on Functionalized Carbon Nanotubes. *J. Phys. Chem. C* **2014**, *118*, 22249-22257.

(50) Nepal, D.; Geckeler, K. E. pH- Sensitive Dispersion and Debundling of Single- Walled Carbon Nanotubes: Lysozyme as a Tool. *Small* **2006**, *2*, 406-412.

(51) Horn, D. W.; Tracy, K.; Easley, C. J.; Davis, V. A. Lysozyme Dispersed Single-Walled Carbon Nanotubes: Interaction and Activity. *J. Phys. Chem. C*, **2012**, *116*, 10341-10348.

(52) Horn, D. W.; Ao, G.; Marsey, M.; Zakri, C.; Poulin, P.; Davis, V. A. Lysozyme-Single Walled Carbon Nanotubes: Dispersion State and Fiber Toughness. *Adv. Funct. Mater.* **2013**, *23*, 6082-6090.

(53) Joseph, D.; Tyagi, N.; Ghimire, A.; Geckeler, K. E. A Direct Route Towards Preparing pH-Sensitive Graphene Nanosheets with Anti-Cancer Activity. *RSC Adv.* **2014**, *4*, 4085-4093.

(54) Calvaresi, M.; Zerbetto, F. In Silico Carborane Docking to Proteins and Potential Drug Targets. *J. Chem. Inf. Model.* **2011**, *51*, 1882-1896.

(55) Mudedla, S. K.; Singam, E. R. A.; Sundar, J. V.; Pedersen, M. N.; Murugan, N. A.; Kongsted, J.; Ågren, H.; Subramanian, V. Enhancement of Internal Motions of Lysozyme through Interaction with Gold Nanoclusters and its Optical Imaging. *J. Phys. Chem. C* **2015**, *119*, 653-664.

(56) Case, D. A.; Cheatham III, T. E.; Darden, T.; Gohlke, H.; Luo, R.; Merz, Jr., K. M.; Onufriev, A.; Simmerling, C.; Wang, B.; Woods, R. The Amber Biomolecular Simulation Programs. *J. Comput. Chem.* **2005**, *26*, 1668-1688.

(57) Kollman, P. A.; Massova, I.; Reyes, C.; Kuhn, B.; Huo, S.; Chong, L.; Lee, M.;

Lee, T.; Duan, Y.; Wang, W. et al. Calculating Structures and Free Energies of Complex Molecules: Combining Molecular Mechanics and Continuum Models. *Acc. Chem. Res.* **2000**, *33*, 889-897.

(58) Miller , III, B. R.; McGee, Jr., T. D.; Swails, J. M.; Homeyer, N.; Gohlke, H.; Roitberg, A. E. *MMPBSA.py*: An Efficient Program for End-State Free Energy Calculations. *J. Chem. Theory Comput.* **2012**, *8*, 3314-3321.

(59) Wang, S.; Humphreys, E. S.; Chung, S.-Y.; Delduco, D. F.; Lustig, S. R.; Wang, H.; Parker, K. N.; Rizzo, N. W.; Subramoney, S.; Chiang, Y. M et al. Peptides with Selective Affinity for Carbon Nanotubes. *Nat. Mater.* **2003**, *2*, 196-200.

(60) Zorbas, V.; Smith, A. L.; Xie, H.; Ortiz-Acevedo, A.; Dalton, A. B.; Dieckmann, G. R.; Draper, R. K.; Baughman, R. H.; Musselman, I. H. Importance of Aromatic Content for Peptide/Single-Walled Carbon Nanotube Interactions. *J. Am. Chem. Soc.* **2005**, *127*, 12323-12328.

(61) Xie, H.; Becraft, E. J.; Baughman, R. H.; Dalton, A. B.; Dieckmann, G. R. Ranking the Affinity of Aromatic Residues for Carbon Nanotubes by Using Designed Surfactant Peptides. *J. Pept. Sci.* **2008**, *14*, 139-151.

(62) Tomasio, S. M.; Walsh, T. R. Modeling the Binding Affinity of Peptides for Graphitic Surfaces. Influences of Aromatic Content and Interfacial Shape. *J. Phys. Chem. C* **2009**, *113*, 8778-8785.

(63) Zheng, L.; Jain, D.; Burke, P. Nanotube-Peptide Interactions on a Silicon Chip. *J. Phys. Chem. C* **2009**, *113*, 3978-3985.

(64) Hirano, A.; Tanaka, T.; Kataura, H.; Kameda, T. Arginine Side Chains as a Dispersant for Individual Single-Wall Carbon Nanotubes. *Chem. Eur. J.*, **2014**, *20*, 4922-4930.

(65) Wu, E.; Coppens, M.-O.; Garde, S. Role of Arginine in Mediating Protein-Carbon Nanotube Interactions. *Langmuir* **2015**, *31*, 5, 1683-1692.

(66) De Leo, F.; Sgrignani, J.; Bonifazi, D.; Magistrato, A. Structural and Dynamic Properties of Monoclonal Antibodies Immobilized on CNTs: A Computational Study. *Chem. Eur. J.* **2013**, *19*, 12281-12293.

(67) Gu, Z.; Yang, Z.; Wang, L.; Zhou, H.; Jimenez-Cruz, C. A.; Zhou, R. The Role of Basic Residues in the Adsorption of Blood Proteins onto the Graphene surface. *Sci. Rep.* **2015**, *5*, 10873.

(68) Canevet, D.; Perez, E. M.; Martin, N. Wraparound Hosts for Fullerenes: Tailored Macrocycles and Cages. *Angew. Chem. Int. Ed.* **2011**, *50*, 9248-9259.

(69) Ikeda, A. Water-Soluble Fullerenes Using Solubilizing Agents, and their Applications. *J. Incl. Phenom. Macrocycl. Chem.* **2013**, *77*, 49-65.

(70) Perez, E. M.; Martin, N. Curves Ahead: Molecular Receptors for Fullerenes Based on Concave-Convex Complementarity. *Chem. Soc. Rev.* **2008**, *37*, 1512-1519.

(71) Mieda, S.; Ikeda, A.; Shigeri, Y.; Shinoda, W. Thermodynamic Stability of [60]Fullerene and γ- Cyclodextrin Complex in Aqueous Solution: Free Energy Simulation. *J. Phys. Chem. C* **2014**, *118*, 12555-12561.

GRAPHICAL TABLE OF CONTENTS